

# A Computational Study on Fluxional Behavior of Group 6 and 7 Transition-metal Complexes of Borane–Lewis Base Adducts

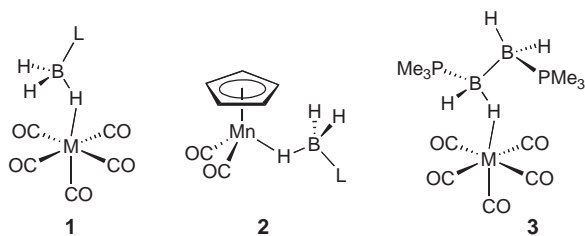
Yasuro Kawano,\* Taeko Kakizawa, Kazunori Yamaguchi, and Mamoru Shimoi\*  
*Department of Basic Science, Graduate School of Arts and Sciences, The University of Tokyo,  
 Meguro-ku, Tokyo 153-8902*

(Received March 1, 2006; CL-060250; E-mail: ckawano1@mail.ecc.u-tokyo.ac.jp, cshimoi@mail.ecc.u-tokyo.ac.jp)

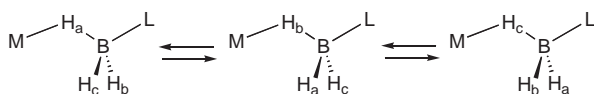
Fluxional behavior of group 6 and 7 metal borane complexes was investigated with use of density functional theory (DFT). Site exchange of BH hydrogen atoms of the borane ligand  $\text{BH}_3 \cdot \text{L}$  or  $\text{B}_2\text{H}_4 \cdot 2\text{PMe}_3$  proceeds via a transition state in which the borane ligand interacts with metal with a bidentate fashion. Calculated values of the activation energy were in good agreement with experimentally observed barriers.

The simplest boron hydride  $\text{BH}_3$  is an unstable species because of the strong Lewis acidity, and readily undergoes coordination of a Lewis base to produce a base adduct,  $\text{BH}_3 \cdot \text{L}$ . Likewise, diborane(4) exists as a bis(base) adduct,  $\text{B}_2\text{H}_4 \cdot 2\text{L}$ . These borane–Lewis base adducts are charge neutral and isoelectronic with alkanes.

Previously, we reported photochemical syntheses of borane  $\sigma$  complexes **1–3**, in which a borane adduct coordinates to metal through a B–H–M three-center two-electron bond (Scheme 1).<sup>1–4</sup> Additionally, we pointed out that these species can be model cases of transient alkane complexes.<sup>5</sup> In the  $^1\text{H}$ NMR spectra, monoborane derivatives **1** and **2** exhibit only one BH proton resonance due to rapid exchange between the bridging and terminal BH hydrogen atoms (Scheme 2).<sup>1,2</sup> The diborane(4) complexes **3** show analogous *geminal* BH hydrogen exchange as well as *vicinal* BH exchange, the latter of which is much slower than the former.<sup>4</sup> For the fluxional process, we proposed a concerted mechanism, in which the metal moiety transfers BH hydrogen atoms via a transition state involving an  $\eta^2$ -interacting borane ligand.<sup>1</sup> To better understand the mechanism, we conducted a DFT study on the dynamic behavior of  $[\text{Cr}(\text{CO})_5(\eta^1\text{-BH}_3 \cdot \text{L})]$  (**1a**:  $\text{L} = \text{NMe}_3$  and **1b**:  $\text{L} = \text{PMe}_3$ ),  $[\text{CpMn}(\text{CO})_2(\eta^1\text{-BH}_3 \cdot \text{L})]$  (**2a**:  $\text{L} = \text{NMe}_3$  and **2b**:  $\text{L} = \text{PMe}_3$ ), and  $[\text{Cr}(\text{CO})_5(\eta^1\text{-B}_2\text{H}_4 \cdot 2\text{PMe}_3)]$  (**3a**).



**Scheme 1.** Fluxional Borane Complexes.  $\text{M} = \text{Cr}$  and  $\text{W}$ ;  $\text{L} = \text{NMe}_3$  and  $\text{PMe}_3$ .



**Scheme 2.**

Geometry optimization was carried out at the DFT/B3LYP level of theory with basis sets LanL2DZ (Cr and Mn) and 6-31G(d) (all others). Vibrational analyses were further performed to characterize the stationary points. Subsequently, on the obtained structures, the energy was calculated at the B3LYP/6-311+G(2d,p) level. Key geometrical parameters of the species are summarized in Table 1.

The optimized structures of **1a**, **1b**, **2a**, **2b**, and **3a** well reproduced their X-ray crystal structures. The long metal–boron separations (2.706–2.966 Å) indicate  $\eta^1$ -coordination mode of the borane ligand. On coordination, the BH bond is stretched only slightly. The bond distances of metal-coordinated BH range from 1.25 to 1.27 Å while those of terminal ones are around 1.20 Å. It was thus confirmed that compounds **1–3** are classified as unstretched  $\sigma$  complexes. This was suggested already based on X-ray structural analyses although there remained uncertainty because of large standard deviations in hydrogen-containing parameters.<sup>1,2</sup>

Transition states (TS) for the BH exchange of **1** and **2** were located as  $\eta^2$ -borane structures with  $C_s$  symmetry. Two of them (**TS1a** and **TS2b**) are illustrated in Figure 1 along with the equilibrium structures of **1a** and **2b**. The activation barriers for the fluxional processes were calculated to be 31.9 and 29.3 kJ mol<sup>−1</sup> for **1a** and **2b**, respectively.<sup>6</sup> They are in good agreement with the experimental values (34 kJ mol<sup>−1</sup> at 253 K and 30 kJ mol<sup>−1</sup> at 213 K) obtained by NMR spectroscopy.<sup>1,2</sup> In the TSs, the coordinated hydrogen atoms are much farther from the central metal than in the stable forms. The metal–hydrogen interatomic distances are 2.428 and 2.225 Å in **TS1a** and **TS2b**, respectively. Importantly, the metal–boron separations in **TS1a** and **TS2b** (2.855 and 2.642 Å, respectively) are roughly the same as those

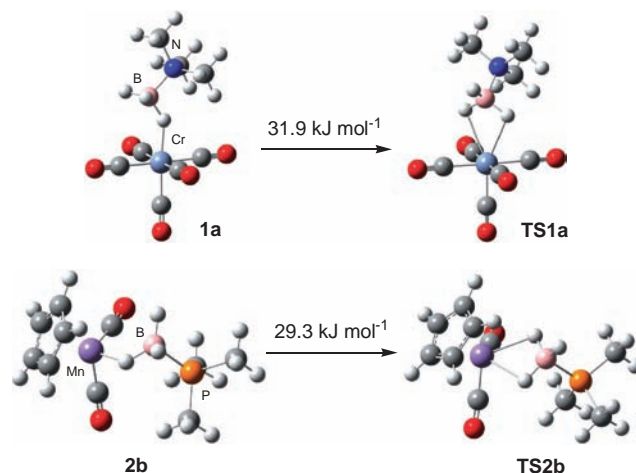


**Figure 1.**

**Table 1.** Selected interatomic distances (Å) and bond angles (deg) of optimized species<sup>a</sup>

Compound	M...B	M-H(brid)	B-H(brid)	B-H(term)	M-H-B
<b>1a</b>	2.910 (2.87(2))	1.806 (—) <sup>b</sup>	1.251 (—) <sup>b</sup>	1.202, 1.203 (—) <sup>b</sup>	144.0 (—) <sup>b</sup>
<b>TS1a</b>	2.855	2.428	1.216	1.207	97.6
<b>1b</b>	2.881 (2.79(1))	1.829 (1.94(10))	1.248 (1.12(11))	1.202, 1.207 (0.94(7), 0.97(17))	138.1 (130(8))
<b>TS1b</b>	2.813	2.391	1.216	1.208	97.1
<b>2a</b>	2.741 (2.682(3))	1.707 (1.65(4))	1.252 (1.19(4))	1.200, 1.208 (1.14(4), 0.99(5))	135.3 (142(3))
<b>TS2a</b>	2.678	2.260	1.214	1.209	95.9
<b>2b</b>	2.706 (2.573(2))	1.709 (1.81(4))	1.251 (1.01(4))	1.212, 1.201 (0.84(4), 1.02(5))	131.5 (129(3))
<b>TS2b</b>	2.642	2.225	1.216	1.209	95.8
<b>3a</b>	2.966 (2.876(8))	1.823 (1.76(8))	1.273 (1.28(8))	1.211 (1.40(9)), <sup>c</sup> 1.226, 1.220 (1.20(7), 1.13) <sup>d</sup>	146.1 (141(8))
<b>TS3ag</b>	2.874	2.386, 2.458	1.229, 1.222	1.220, 1.228 <sup>d</sup>	100.4, 97.0
<b>TS3av</b>	3.522	2.703	1.225	1.225	122.9

<sup>a</sup>Parameters obtained by X-ray diffraction are shown in parentheses. <sup>b</sup>The BH protons could not be located in X-ray studies. <sup>c</sup> $\alpha$ -BH<sub>term</sub>. <sup>d</sup> $\beta$ -BH<sub>term</sub>.

of **1a** and **2b**. Thus, during the exchange process, the metal moiety migrates as if it pivots upon the boron atom to leave hitherto coordinated hydrogen, approaching another BH. In consideration of such a structural change, it should be probable that the activation barriers virtually correspond to the energy to weaken the bridging hydrogen–metal interaction. Note that the M–H and M...B interatomic distances are also considerably longer in comparison to those in  $\eta^2$ -borohydride<sup>7</sup> and  $\eta^2$ -borane–Lewis base adduct complexes.<sup>8,9</sup> For example, the corresponding bond lengths of [N(PPh<sub>3</sub>)<sub>2</sub>][Cr(CO)<sub>4</sub>( $\eta^2$ -BH<sub>4</sub>)] are 1.96(7), 1.80(6) (Cr–H), and 2.29(1) (Cr...B) Å,<sup>7b</sup> and those of [Cp\*Ru( $\eta^2$ -BH<sub>3</sub>·PPh<sub>2</sub>CH<sub>2</sub>PPh<sub>2</sub>)] [PF<sub>6</sub>] are 1.61(4), 1.70(3) (Ru–H), and 2.180(4) (Ru...B) Å.<sup>8a</sup> The geometries of the TSs are reminiscent of the TS for CH exchange of a short-lived tungsten–methane complex [W(CO)<sub>5</sub>(CH<sub>4</sub>)], which involves  $\eta^2$ -interacting methane with long CH...W and C...W separations.<sup>10</sup> The values of activation energy for the dynamic process of all the calculated compounds are listed in Table 2.

Figure 2 depicts DFT-optimized structures of **3a** and TSs for two types of BH exchange. **TS3ag** and **TS3av** correspond to the TSs for *geminal* and *vicinal* BH exchange, respectively. For those processes, the activation energies were evaluated to be 30.7 and 53.7 kJ mol<sup>−1</sup>, respectively, in accordance with experimental values.<sup>4</sup> **TS3ag** has a structure essentially similar to **TS1b** except the presence of a BH<sub>2</sub>·PMe<sub>3</sub> group on boron. In **TS3av**, the diborane ligand interacts with metal through two

*vicinal* BH protons to form a five-membered transition state. The two bridging hydrogen atoms are much more distant (2.703 Å) from the Cr atom than in **3a** (1.823 Å). On transformation from **3a** to **TS3av**, the metal fragment moves so that it may separate greatly from  $\alpha$ -BH, and it approaches the  $\beta$ -BH moiety to form the symmetrical (C<sub>2</sub>) structure. This large deformation should be responsible for the high barrier for the *vicinal* hydrogen exchange. The M...B and M–H interatomic distances are significantly longer than those of stable  $\eta^2$ -diborane(4) complexes [M(CO)<sub>4</sub>( $\eta^2$ -B<sub>2</sub>H<sub>4</sub>·2PMe<sub>3</sub>)] (M = Cr and W; where M–H = 1.80–1.91 Å and M...B = 2.412(8)–2.54(2) Å).<sup>3</sup> The dynamic behavior of **3a** is parallel to theoretically predicted properties of [W(CO)<sub>5</sub>(C<sub>2</sub>H<sub>6</sub>)], in which *vicinal* CH exchange requires higher activation energy relative to *geminal* exchange.<sup>10</sup> It is also akin to solution behavior of [CpRe(CO)<sub>2</sub>(*cyclo*-C<sub>5</sub>H<sub>10</sub>)].<sup>11</sup> This only NMR-observable alkane complex shows rapid exchange between *geminal* CH protons at −100 °C.

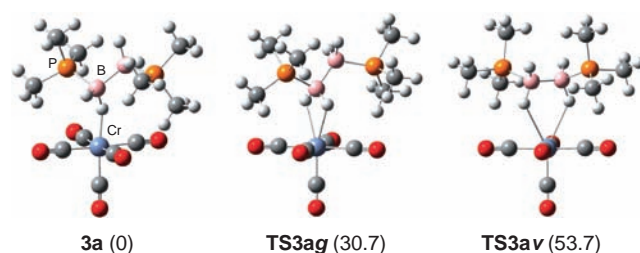
This work was financially supported by the Ministry of Education, Culture, Sports, Science and Technology of Japan [Grant-in-Aid for Special Project Research (No. 15036215)].

#### References and Notes

- M. Shimoi, S. Nagai, M. Ichikawa, Y. Kawano, K. Katoh, M. Uruichi, H. Ogino, *J. Am. Chem. Soc.* **1999**, *121*, 11704.
- T. Kakizawa, Y. Kawano, M. Shimoi, *Organometallics* **2001**, *20*, 3211.
- a) K. Katoh, M. Shimoi, H. Ogino, *Inorg. Chem.* **1992**, *31*, 670. b) M. Shimoi, K. Katoh, H. Ogino, *J. Chem. Soc., Chem. Commun.* **1990**, 811.
- M. Shimoi, K. Katoh, Y. Kawano, G. Kodama, H. Ogino, *J. Organomet. Chem.* **2002**, *659*, 102.
- C. Hall, R. N. Perutz, *Chem. Rev.* **1996**, *96*, 3125.
- For the manganese systems, another saddle point, in which the  $\eta^2$ -borane ligand had turned to the contrary with **TS2** (NMe<sub>3</sub> or PMe<sub>3</sub> is located at the same side with the Cp ligand with respect to the four-membered ring composed of manganese, boron, and two bridging hydrogen atoms), was found. However, they are 19.2 (L = NMe<sub>3</sub>) or 16.0 (L = PMe<sub>3</sub>) kJ mol<sup>−1</sup> further higher relative to the TSs.
- For example: a) Y. Kawano, M. Shimoi, *Chem. Lett.* **1998**, 935. b) M. Y. Darensbourg, R. Bau, M. W. Marks, R. R. Burch, Jr., J. C. Deaton, S. Slater, *J. Am. Chem. Soc.* **1982**, *104*, 6961. c) T. J. Marks, J. R. Kolb, *Chem. Rev.* **1977**, *77*, 263.
- a) N. Merle, G. Kociok-Köhn, M. F. Mahon, C. G. Frost, G. D. Ruggerio, A. S. Weller, M. C. Willis, *Dalton Trans.* **2004**, 3883. b) N. Merle, C. G. Frost, G. Kociok-Köhn, M. C. Willis, A. S. Weller, *J. Organomet. Chem.* **2005**, *690*, 2829.
- a) M. Ingleson, N. J. Patmore, G. D. Ruggiero, C. G. Frost, M. F. Mahon, M. C. Willis, A. S. Weller, *Organometallics* **2001**, *20*, 4434. b) O. Volkov, R. Macías, N. P. Rath, L. Barton, *Inorg. Chem.* **2002**, *41*, 5837.
- S. Zarić, M. B. Hall, *J. Phys. Chem. A* **1997**, *101*, 4646.
- S. Geftakis, G. E. Ball, *J. Am. Chem. Soc.* **1998**, *120*, 9953.

**Table 2.** Activation barriers (kJ mol<sup>−1</sup>) for the BH exchange

Compound	Calculated	Experimental
<b>1a</b>	31.9	34 (213 K)
<b>1b</b>	23.6	<28 (193 K)
<b>2a</b>	36.2	40 (253 K)
<b>2b</b>	29.3	30 (213 K)
<b>3a (geminal)</b>	30.7	28 (173 K)
<b>3a (vicinal)</b>	53.7	64 (285 K)

**Figure 2.** Relative energies are given in kJ mol<sup>−1</sup>.